Available online at www.sciencedirect.com
SCIENCE DIRECT®
Journal of Hydrology 276 (2003) 71–88
Journal of Hydrology
www.elsevier.com/locate/jhydrol

A quantitative approach to aquifer vulnerability mapping

L.D. Connell*, Gerd van den Daele

Department of Earth Sciences, University College London, Gower Street, London WC1E 6BT, UK

Received 18 March 2002; accepted 20 January 2003

Abstract

This paper presents a procedure for calculating the transport to groundwater of surface-released contaminants. The approach is derived from a series of analytical and semi-analytical solutions to the advection–dispersion equation that include root zone and unsaturated water movement effects on the transport process. The steady-state form of these equations provides an efficient means of calculating the maximum concentration at the watertable and therefore has potential for use in vulnerability mapping. A two-layer approach is used in the solutions to represent the unsaturated profile, with the root zone corresponding to the upper layer where evapotranspiration can occur and transport properties can be in contrast to the rest of the profile. A novel transformation is applied to the advection–dispersion equation that considerably simplifies the way in which water movement is represented. To provide a combined flow and transport model an approximate procedure for water movement, using averages of the infiltration and transpiration rates with a novel, simple, quasi-steady state solution, is presented that can be used in conjunction with the solutions to the advection–dispersion equation. This quasi-steady state approximation for water movement allows for layering in the soil profile and root water uptake. Results from the combined quasi-steady state water movement and semi-analytical solute transport procedure compare well with numerical solutions to the coupled unsaturated flow and solute transport equations in a series of hypothetical simulations.

Keywords: Vulnerability mapping; Unsaturated solute transport; Advection–dispersion equation; Analytical solutions

1. Introduction

Mapping the vulnerability of aquifers to pollution involves estimating the potential for contaminants to migrate from the land surface through the unsaturated zone to groundwater throughout areas of interest. Existing vulnerability maps tend to use simple qualitative indices (e.g. the GOD index (Foster, 1987) and the DRASTIC index (Aller et al., 1987)) that bring together key factors believed to influence the solute transport process. At the time the maps were developed this was an appropriate compromise since quantitative information on the various transport properties was largely unavailable and the approach had to be compatible with the cost effective production of maps. Nevertheless vulnerability maps have proved popular tools and are now a common feature of groundwater environmental management throughout the world. However, the various indices used to generate these maps are largely conceptual (and thus subjective), and in general do not differentiate between contaminants.

* Corresponding author. Tel.: +61-39259-6814; fax: +61-39259-6900.
E-mail address: luke.connell@csiro.au (L.D. Connell).

0022-1694/03/$ - see front matter © 2003 Elsevier Science B.V. All rights reserved.
doi:10.1016/S0022-1694(03)00038-6

Nomenclature

a_{i1}, a_{i2}, a_{i3}	constants of integration for Eq. (12) for layer i
b_{i1}, b_{i2}	constants defined by Eq. (13) for layer i
b'_{i1}, b'_{i2}	steady-state form of b_{i1}, b_{i2}
c	solute concentration (M/L^3)
c_s	surface concentration (M solute/L^3)
c_L	concentration at watertable (M solute/L^3)
D	dispersion coefficient equal to $D_m + \alpha_L \lvert q/\theta \rvert$(L^2/T)
D_m	diffusion coefficient (L^2/T)
f	transformed solute concentration (M solute/L^3)
f_{oi}	initial value of f for layer i (M solute/L^3)
h	matric potential (L)
h_g	van Genuchten scale parameter (L)
h_L	matric potential at the profile base (L)
$K(h)$	unsaturated hydraulic conductivity (L^{3}water/L^2/T)
K_d	distribution coefficient (L^3/M soil)
K_s	saturated hydraulic conductivity (L^3 water/L^2/T)
L	depth to watertable (L)
m_s	adsorbed mass (M solute/M soil)
n, m	van Genuchten shape parameter
q	water flux (L^3 water/L^2/T)
Q	transformed depth (L^3 water/L^2)
Q'	transformed Q (L^3 water/L^2)
q_o	temporal average of infiltration (L^3 water/L^2/T)
q_c	solute mass flux (M solute/L^2/T)
q_{co}	constant surface flux of solute (M solute/L^2/T)
R_f	retardation factor
s	Laplace transform variable
S_w	sink/source of water (L^{3}water/L^3/T)
S_{wa}	average sink/source of water (L^{3}water/L^3/T)
t	time parameter (T)
z	vertical coordinate (L)
z_{av}	depth constant (L)
z_{di}	depth of layer i base (L)
z_L	depth of the profile (L)
$\alpha_i, \beta_i, \gamma_i$	equation coefficients for Eq. (10)
α_g	Gardner shape parameter (1/L)
α_L	dispersivity (L)
$\Delta Q_1, \Delta Q_2$	thickness in Q space of layer one and two (L^{3}water/L^2)
θ	volumetric water content (L^{3}water/L^3)
θ_s	saturated volumetric water content (L^{3}water/L^3)
θ_r	residual volumetric water content (L^{3}water/L^3)
μ	degradation rate (T^{-1})
ρ	soil dry bulk density (M soil/L^3)

A number of alternatives to the vulnerability indices have been developed that are based on the physics of solute transport. Initially developed for ranking hazardous chemicals such as pesticides, these approaches also have potential for use in vulnerability mapping (Khan and Liang, 1989). One example is the attenuation factor (Rao et al., 1985), a physically based index that allows for degradation, the recharge flux, and adsorption. Other work has taken this further to develop relations for the residual mass fraction of a pesticide that arrives at the watertable by solving the advection–dispersion equation (Hantush et al., 2000). All these approaches could potentially be used within geographical information systems (GIS) to allows users to interactively generate contaminant specific vulnerability maps, an important development that would allow improved management of water resources and land use. A key requirement for such an application is that the indices be relatively simple to calculate, since such maps involve numerous calculations of the index over the mapping area.

Another approach to vulnerability mapping would be to calculate the probability that a contaminant released at surface would arrive at the watertable above the regulatory limit for groundwater for that compound. This probability could then be mapped. This risk calculation would require the combination of a solution to the advection–dispersion equation with a treatment of parameter uncertainty. While there are several packages that provide numerical solutions to this equation (Wagenet and Hutson, 1986; Leonard et al., 1987) these would be difficult to incorporate

within a GIS and still provide a tractable system for interactive map generation since numerous simulations could be required to generate a map. This problem would be exacerbated if the inherent parameter uncertainties had to also be treated, perhaps through Monte Carlo analysis, within the GIS. This paper presents an approach for calculating the contaminant risk that would be suitable for use in an interactive fashion within a GIS.

As an alternative to numerical solutions, the advection–dispersion equation can also be solved analytically. However, the derivation of analytical solutions must be able to include the effect of a range of processes. One important process for a field soil exposed to climate is the variation in water content and flux both spatially and through time. In addition, many soils exhibit a biologically active zone, roughly corresponding to the root zone, where the organic content and oxygen concentration are higher than deeper in the profile (Jury and Grsruber, 1989). For many contaminants this biologically active zone will mean that degradation and retardation rates are higher than deeper in the profile. In addition to vertical differences in transport properties, there can be a contrast in soil hydraulic properties. Also, solute concentrations may be affected by the uptake of water by plants, increasing if the plant roots exclude the solutes.

However, in order for the mathematical problem to be tractable analytically, existing solutions tend to involve a number of approximations about the manner in which the physical system is represented. Approximations made in order to solve the advection–dispersion equation have been constant coefficients (Elrick et al., 1994; Sun et al., 1999; Connell and Haverkamp, 1996) or coefficients that are time varying but constant with respect to position (Barry and Sposito, 1989). For transport in the unsaturated zone spatially constant coefficients means that retardation, degradation and dispersion are constant throughout the unsaturated profile and therefore any contrast between root zone properties and the rest of the profile is not represented. The constant coefficient assumption also means that the vertical and transient variation in the unsaturated water content observed under field conditions cannot represented. Bosma and van der Zee (1992) present a solution that allows for layering using a travelling wave approximation to simplify the transport equation. Connell (2002) allowed for root zone effects by treating the root zone processes in a lumped fashion and combining this with an analytical solution for below root zone transport.

A complication often encountered in field soils is the existence of macropores that allow preferential flow of water and rapid transport of solute. This preferential transport can be further complicated by the diffusional transport of solutes from the macropore into the surrounding soil matrix. While the solutions discussed in the preceding paragraph have considered that the transport behaves as that in porous media, other approaches exist for some of the dual porosity systems encountered with preferential flow (e.g. Hantush et al., 2002; van Genuchten and Dalton, 1986). As a first analysis in this paper we consider the transport to behave as that in a porous medium.

In this paper, analytical and semi-analytical solutions to the advection–dispersion equation are presented that have potential for use in mapping the risk of surface released contamination to groundwater systems. In the first part of the paper semi-analytical solutions are derived that allow for a contrast between root zone and sub-root zone properties, and variation in the vertical unsaturated water content. These solutions use a spatially transformed advection–dispersion equation that simplifies the way in which water movement is represented. With this transformed equation a quasi-steady state approximation for the water movement is developed that allows for layering in soil hydraulic properties and uses temporal averages of the infiltration and evapo-transpiration rates. The accuracy of this approximation when there is transient variation in unsaturated water movement is investigated in a series of hypothetical simulations with the numerical unsaturated flow and transport model SWIMv2 (Verburg et al., 1996) as a basis of comparison. These simulations involve a time series in the surface boundary conditions where discrete infiltration events are interspersed with periods of transpiration. In a second part to the paper steady-state forms of the semi-analytical solutions are derived that have potential for use in the generation of GIS-based risk maps.

The solutions are derived for two situations; where there is a finite profile bounded by the soil surface and

the watertable and where the profile is semi-infinite, with the soil surface being the upper boundary.

2. Mathematical derivation

2.1. The advection–dispersion equation and its transformation

The advection–dispersion equation is derived by combining the solute mass flux relation with conservation of mass. Conservation of solute mass may be written as,

$$\frac{\partial(c\theta)}{\partial t} + \rho\frac{\partial m_s}{\partial t} = -\frac{\partial q_c}{\partial z} + \mu\theta c \quad (1)$$

With Eq. (1) degradation only occurs in the dissolved solute phase, not the adsorbed. The solute mass flux, q_c, combines the effects of solute advection and dispersion and can be written as,

$$q_c = -\theta D\frac{\partial c}{\partial z} + qc \quad (2)$$

where D is the dispersion coefficient equal to $D_m + \alpha_L|q/\theta|$.

Introducing Eq. (2) into Eq. (1) leads to,

$$\frac{\partial(c\theta)}{\partial t} + \rho\frac{\partial m_s}{\partial t} = \frac{\partial}{\partial z}\left[\theta D\frac{\partial c}{\partial z}\right] - \frac{\partial(qc)}{\partial z} + \mu\theta c \quad (3)$$

Eq. (3) is the advection–dispersion equation for solute transport in unsaturated soil.

With a linear adsorption isotherm ($m_s = K_d c$) and continuity of water mass, Eq. (3) becomes,

$$\theta R_f\frac{\partial c}{\partial t} = \frac{\partial}{\partial z}\left[\theta D\frac{\partial c}{\partial z}\right] - q(z,t)\frac{\partial c}{\partial z} + (\mu\theta - S_w)c \quad (4)$$

where $R_f = 1 + K_d\rho/\theta$ and S_w represents water loss due to transpiration. In Eq. (4) solute is excluded from the water taken up by the plant root system for transpiration and that loss of water mass represented by S_w acts to increase the solute concentration. However, if solute is taken up into the plant roots with the transpiration water at the same rate, than S_w does not appear in Eq. (4) as the solute concentration is unaffected, even though the mass decreases (through reductions in the volumetric water content, θ).

Bond and Smiles (1983) transformed the advection–dispersion equation by introducing the following variable,

$$Q = \int_0^z \theta\,d\bar{z} \quad (5)$$

Here this transform is extended to the following,

$$Q = \int_0^z \theta R_f\,d\bar{z} \quad (6)$$

and used to transform Eq. (4) leading to

$$\frac{\partial f}{\partial t} = \frac{\partial}{\partial Q}\left[R_f\theta^2 D\frac{\partial f}{\partial Q}\right] - \left[q(0,t) + \int_o^z S_w\,d\bar{z}\right]\frac{\partial f}{\partial Q} + \frac{(\mu\theta - S_w)}{R_f\theta}f \quad (7)$$

where $f(Q,t)$ is the Q space form of the concentration, $c(z,t)$.

Without plant water uptake Eq. (7) becomes,

$$\frac{\partial f}{\partial t} = \frac{\partial}{\partial Q}\left[R_f\theta^2 D\frac{\partial f}{\partial Q}\right] - q(0,t)\frac{\partial f}{\partial Q} + \frac{\mu}{R_f}f \quad (8)$$

2.2. Two-layer semi-analytical solution

2.2.1. Physical approximations

For many soil profiles it may be a reasonable approximation to assume that there is a compact root zone with more or less uniform root distribution, and thus vertically uniform plant water uptake, S_w. Therefore for the first of the two layers in our model, S_w could be approximated by a spatial constant within the layer. For the second layer, below the root zone, S_w is zero. For the first layer $\int_o^z S_w(t)d\bar{z}$ can be integrated to $S_w(t)z$. Since $S_w(t)z$ acts to reduce the advective water flux in Eq. (7) replacing z by a constant, z_{av}, would mean that advective transport is overestimated above z_{av} and underestimated below that point. z_{av} could be chosen to ensure the travel time through the root zone is preserved, even though it is not accurately represented within the layer.

In an extension of the transform used by Barry and Sposito (1989), $Q' = Q - \int_o^t [q(0,\bar{t}) + S_w(\bar{t})z_{av}]\,d\bar{t}$, can be substituted into Eq. (7), leading to,

$$\frac{\partial f'}{\partial t} = \frac{\partial}{\partial Q'}\left[R_f\theta^2 D\frac{\partial f'}{\partial Q'}\right] + \frac{\mu\theta - S_w}{\theta R_f}f' \quad (9)$$

where f' is the Q' transform of f presented in Eq. (7). This transformation removes the advective term from Eq. (7) and redefines the problem in a moving boundary form. While Eq. (9) does not form the basis for the solutions presented below, it does demonstrate that the advective component of transport, at a given time, is determined by the cumulative or net surface water flux up to that time, $\int_o^t q(0,\bar{t})\,\mathrm{d}\bar{t}$ and the cumulative transpiration, $\int_o^t S_w(\bar{t})\,\mathrm{d}\bar{t}$. To find the concentration at a time, $q_o t$ and $S_{wa}t$ can replace the integral terms in the previous sentence, where q_o and S_{wa} are averages. Setting aside water content effects, solute transport could then be modeled using readily available information on the surface water fluxes (readily measured as cumulatives) rather than simultaneous solution of the water movement equation.

However, while the advective component of transport can largely be described using averages of the surface water flux and root water uptake, in order to map a location in to the Q transform space the water content profile is required. In an unsaturated soil the water content will vary with depth. At equilibrium, with a zero water flux, the water content profile above the watertable will be equivalent to the matric potential relationship, with the negative of the distance above the watertable being equivalent to the matric potential. The water content therefore tends to saturation with depth towards the watertable. Consistent with our average surface flux approximation is that water movement is in a quasi-steady state. While this may seem a coarse approximation for a soil exposed to climate, transient water movement responses are damped by the soil profile. As a result, the water movement behaviour approaches an averaged state with depth. This will be sensitive to both the climate and soil hydraulic properties. Under steady state conditions simple relationships can be derived for the water content profile with respect to the surface flux (i.e. Gardner, 1958).

2.2.2. Derivation of layer equation

The approach presented here involves conceptualising the profile as being composed of two layers. Towards the surface there is a biologically active zone, where rates of degradation and adsorption are higher than deeper in the profile, and where there is plant water uptake through the root system.

Eq. (7) is used to describe solute transport within the root zone and Eq. (8) for below the root zone. Within each layer a constant coefficient form of the differential equations is solved analytically in Laplace space. These layer analytical solutions are then coupled together to provide a description for the dependent variable in Laplace space over the problem domain. Numerical Laplace inversion is then used to calculate values for the dependent variable at locations in time.

A generalised form of the transformed constant coefficient approximation for Eqs. (7) and (8) is presented below,

$$\frac{\partial f_i}{\partial t} = \alpha_i \frac{\partial^2 f_i}{\partial Q_i^2} - \beta_i \frac{\partial f_i}{\partial Q_i} + \gamma_i f_i \tag{10}$$

where i refers to the layer number and $\alpha_i = \langle R_f \theta^2 D\rangle_i$, $\beta_i = (q_{oi} + S_{wai} z_{avi})$, $\gamma_i = (\mu_i \langle\theta_i\rangle - S_{wai})/\langle R_{fi}\theta_i\rangle$, and where S_{wa2} is zero. The brackets $\langle\ \rangle$ refer to layer constant values. In Eq. (10) Q_i is defined as being local to each layer; i.e. $Q_i = \int_{z_{di}}^{z} \theta R_{fi}\mathrm{d}\bar{z}$, where z_{di} is the depth of the interface between the two layers, for example, $z_{d1} = 0$ and z_{d2} is the depth of the interface between the two layers.

Taking the Laplace transform of Eq. (10) leads to the following equation,

$$s\bar{f}_i - f_{oi} = \alpha_i \frac{\mathrm{d}^2 \bar{f}_i}{\mathrm{d}Q_i^2} - \beta_i \frac{\mathrm{d}\bar{f}_i}{\mathrm{d}Q_i} + \gamma_i \bar{f}_i \tag{11}$$

where f_{oi} refers to the initial value of f, in this case a constant.

The analytical solution to Eq. (11) is of the following form,

$$\bar{f}_i = a_{i1} e^{b_{i1} Q_i} + a_{i2} e^{b_{i2} Q_i} + a_{i3} \tag{12}$$

Substituting Eq. (12) into (11) leads to the following,

$$b_{i1} = \frac{\beta_i - \sqrt{\beta_i^2 + 4\alpha_i(s-\gamma_i)}}{2\alpha_i} \quad \text{and}$$

$$b_{i2} = \frac{\beta_i + \sqrt{\beta_i^2 + 4\alpha_i(s-\gamma_i)}}{2\alpha_i} \quad \text{and} \tag{13}$$

$$a_{i3} = f_{io}/(s-\gamma_i).$$

The coefficients a_{i1} and a_{i2} are determined from coupling the equations for each layer (defined by

Eq. (12)) together and introducing the boundary conditions.

2.2.3. Finite domain: surface to watertable

2.2.3.1. Prescribed surface concentration. Surface concentration;

$$c(0,t) = c_s(t)$$

or in Laplace transform space, $\bar{f}(Q_1 = 0) = \bar{c}_s(s)$.With the above condition and using Eq. (12) defined for the first layer,

$$a_{11} = \bar{c}_s - a_{12} - a_{13} \tag{14}$$

For the lower boundary conditions;

$$c(L,t) = c_L(t)$$

which leads to,

$$a_{21} = \left[\bar{c}_L - a_{23} - a_{22}e^{b_{22}\Delta Q_2}\right]/e^{b_{21}\Delta Q_2} \tag{15}$$

In order to solve the dependent variable variation throughout the problem domain the two layer equations need to be linked together. The conditions applied to link the equations are continuity of mass and dependent variable across the interface between layers 1 and 2.

Continuity of dependent variable is expressed as $\bar{f}_1(Q_1 = \Delta Q_1) = \bar{f}_2(Q_2 = 0)$, and with Eqs. (12),(14) and (15), this leads to,

$$\begin{aligned} &a_{12}\left[e^{b_{12}\Delta Q_1} - e^{b_{11}\Delta Q_1}\right] + a_{22}\left[e^{(b_{22}-b_{21})\Delta Q_2} - 1\right] \\ &\quad = \left[\bar{c}_L - a_{23}\right]e^{-b_{21}\Delta Q_2} - \left[\bar{c}_s - a_{13}\right]e^{b_{11}\Delta Q_1} + a_{23} - a_{13} \end{aligned} \tag{16}$$

Continuity of solute mass in Laplace transform space can be written as,

$$\bar{q}_{c1}(Q_1 = \Delta Q_1) = \bar{q}_{c2}(Q_2 = 0)$$

or with Eq. (2) in Q space,

$$\begin{aligned} &\left[-[R_f\theta^2 D]\frac{d\bar{f}_1}{dQ_1} + q\bar{f}_1\right]_{Q_1=\Delta Q_1} \\ &= \left[-[R_f\theta^2 D]\frac{d\bar{f}_2}{dQ_2} + q\bar{f}_2\right]_{Q_2=0} \end{aligned} \tag{17}$$

Substitution of Eqs. (12),(14) and (15), and noting that $(q\bar{f}_1)_{Q_1=\Delta Q_1} = (q\bar{f}_2)_{Q_2=0}$ leads to,

$$\begin{aligned} &a_{12}[R_f\theta^2 D]_1[b_{11}e^{b_{11}\Delta Q_1} - b_{12}e^{b_{12}\Delta Q_1}] \\ &\quad + a_{22}[R_f\theta^2 D]_2[b_{22} - b_{21}e^{(b_{22}-b_{21})\Delta Q_2}] \\ &\quad = [a_{23} - \bar{c}_L][R_f\theta^2 D]_2 b_{21}e^{-b_{21}\Delta Q_2} \\ &\quad + [\bar{c}_s - a_{13}][R_f\theta^2 D]_1 b_{11}e^{b_{11}\Delta Q_1} \end{aligned} \tag{18}$$

Eqs. (16) and (18) can be solved for the two unknowns, a_{12} and a_{22} which can then be used to find a_{11} and a_{21} using Eqs. (14) and (15). For ease of notation Eq. (16) can be rewritten as,

$$a_{22}K_1 + a_{12}K_2 = K_3 \tag{19}$$

and Eq. (18) as

$$a_{12}L_1 + a_{22}L_2 = L_3 \tag{20}$$

where the K's can be found by matching terms in Eq. (19) with those in Eq. (16) and the L's by matching Eq. (20) with Eq. (18).

Solving Eqs. (19) and (20) yields,

$$a_{12} = \frac{L_3 - K_3L_2/K_1}{L_1 - K_2L_2/K_1} \tag{21}$$

and

$$a_{22} = \frac{[K_3 - a_{12}K_2]}{K_1} \tag{22}$$

2.2.3.2. Prescribed surface flux. Expressions for Eq. (12)'s coefficients can also be calculated for when there is a fixed flux of solute at the surface, q_{co}, starting with the following definition,

$$\bar{q}_{co} = \left[-[R_f\theta^2 D]\frac{d\bar{f}}{dQ} + q\bar{f}\right]_{Q=0} \tag{23}$$

Substitution of Eq. (12) for layer 1 leads to

$$\begin{aligned} \bar{q}_{co} &= a_{11}(q_{o1} - [R_f\theta^2 D]_1 b_{11}) \\ &\quad + a_{12}(q_{o1} - [R_f\theta^2 D]_1 b_{12}) + q_{o1}a_{13} \end{aligned} \tag{24}$$

with the layer definitions for water content and dispersivity.Or in terms of a_{11},

$$\begin{aligned} a_{11} &= [\bar{q}_{co} - a_{12}(q_{o1} - [R_f\theta^2 D]_1 b_{12}) \\ &\quad - q_{o1}a_{13}]/(q_{o1} - [R_f\theta^2 D]_1 b_{11}) \end{aligned} \tag{25}$$

Substitution of a_{11} into the expressions for flux and

dependent variable continuity leads to the following,

$$K_1 = [R_f\theta^2 D]_2[b_{21}e^{(b_{22}-b_{21})\Delta Q_2} - b_{22}] \quad (26)$$

$$K_2 = [R_f\theta^2 D]_1 \times\left[b_{12}e^{b_{12}\Delta Q_1} - b_{11}e^{b_{11}\Delta Q_1}\frac{q_{o1} - [R_f\theta^2 D]_1 b_{12}}{q_{o1} - [R_f\theta^2 D]_1 b_{11}}\right]$$

$$K_3 = (\bar{c}_L - a_{23})e^{-b_{21}\Delta Q_2}b_{21}[R_f\theta^2 D]_2 - \frac{\bar{q}_{co} - q_{o1}a_{13}}{q_{o1} - [R_f\theta^2 D]_1 b_{11}}b_{11}[R_f\theta^2 D]_1 e^{b_{11}\Delta Q_1}$$

$$L_1 = e2^{b_{12}\Delta Q_1} - \frac{q_{o1} - [R_f\theta^2 D]_1 b_{12}}{q_{o1} - [R_f\theta^2 D]_1 b_{11}}e^{b_{11}\Delta Q_1}$$

$$L_3 = a_{23} - a_{13} - \frac{q_{co} - q_{o1}a_{13}}{q_{o1} - [R_f\theta^2 D]_1 b_{11}}e^{b_{11}\Delta Q_1} + (\bar{c}_L - a_{23})e^{-b_{21}\Delta Q_2}$$

where L_2 is the same definition as for the constant concentration surface boundary condition.

2.2.4. Semi-infinite domain

While the two-layer solution presented above was for the finite domain bounded by the soil surface and the watertable, a two-layer solution can also be derived for an semi-infinite domain for the lower layer. From Eq. (12), the solution in Laplace space for layer one is,

$$\bar{f}_1 = a_{11}e^{b_{11}Q_1} + a_{12}e^{b_{12}Q_1} + a_{13} \quad (27)$$

and for layer two,

$$\bar{f}_2 = a_{21}e^{b_{21}Q_2} + a_{23} \quad (28)$$

where

$$b_{11} = \frac{\beta_1 - \sqrt{\beta_1^2 + 4\alpha_1(s-\gamma_1)}}{2\alpha_1},$$

$$b_{12} = \frac{\beta_1 + \sqrt{\beta_1^2 + 4\alpha_1(s-\gamma_1)}}{2\alpha_1}, \quad (29)$$

$$b_{21} = \frac{\beta_2 - \sqrt{\beta_2^2 + 4\alpha_2(s-\gamma_2)}}{2\alpha_2} \text{ and}$$

$a_{13} = f_{1o}/(s-\gamma_1)$, $a_{23} = f_{2o}/(s-\gamma_2)$.

For a Dirichlet boundary condition and applying conditions of flux and concentration continuity across the boundary between layer one and two leads to,

$$a_{21} = \frac{[R_f\theta^2 D]_1\{(a_{13}-a_{23})(b_{11}e^{b_{11}\Delta Q_1} - b_{12}e^{b_{12}\Delta Q_1}) + e^{\Delta Q_1 b_{12} + \Delta Q_1 b_{11}}(\bar{C}_o - a_{13})(b_{11} - b_{12})\}}{e^{\Delta Q_1 b_{11}}([R_f\theta^2 D]_1 b_{11} - [R_f\theta^2 D]_2 b_{21}) + e^{\Delta Q_1 b_{12}}([R_f\theta^2 D]_2 b_{21} - [R_f\theta^2 D]_1 b_{12})} \quad (30)$$

or substituted into Eq. (28) and for zero initial conditions,

$$\bar{f}_2(Q_2, s) = \frac{[R_f\theta^2 D]_1 \bar{C}_o(b_{11} - b_{12})e^{\Delta Q_1(b_{12}+b_{11}) + b_{21}Q_2}}{e^{\Delta Q_1 b_{11}}([R_f\theta^2 D]_1 b_{11} - [R_f\theta^2 D]_2 b_{21}) + e^{\Delta Q_1 b_{12}}([R_f\theta^2 D]_2 b_{21} - [R_f\theta^2 D]_1 b_{12})} \quad (31)$$

where ΔQ_1 is the thickness of the root zone layer.

For a prescribed flux and zero initial conditions,

$$\bar{f}_2(Q_2, s) = \frac{\bar{q}_{co}e^{\Delta Q_1 b_{11} + b_{21}Q_2}[\Omega - b_{11}]}{(q_{o1} - [R_f\theta^2 D]_1 b_{11})\left[\Omega - \frac{[R_f\theta^2 D]_2 b_{21}}{[R_f\theta^2 D]_1}\right]} \quad (32)$$

where

$$\Omega = \frac{b_{12}e^{b_{12}\Delta Q_1}[q_{o1} - [R_f\theta^2 D]_1 b_{11}] - b_{11}e^{b_{11}\Delta Q_1}[q_{o1} - [R_f\theta^2 D]_1 b_{12}]}{e^{b_{12}\Delta Q_1}[q_{o1} - [R_f\theta^2 D]_1 b_{11}] - e^{b_{11}\Delta Q_1}[q_{o1} - [R_f\theta^2 D]_1 b_{12}]} \quad (33)$$

2.3. Steady-state concentration

Eqs. (31) or (32) could be used with numerical Laplace inversion to calculate the concentration through time at the watertable depth and thus the time at which regulatory limits (for example) are exceeded. Another approach would be to calculate the steady-state concentration and use this with a treatment of parameter uncertainty to estimate

the maximum risk posed by a contaminant source. By definition,

$$f_{2STD}(Q_2) = \lim_{s\to 0}[s\bar{f}_2(Q_2, s)] \tag{34}$$

where f_{2STD} is f_2 at steady-state. With Eqs. (31) and (34), and $\bar{C}_o = C_o/s$ (a constant concentration at the surface) f_{2STD} can be defined,

$$f_{2STD}(Q_2) = \frac{[R_f\theta^2 D]_1 C_o(b'_{11} - b'_{12})e^{\Delta Q_1(b'_{12}+b'_{11})+b'_{21}+Q_2}}{e^{\Delta Q_1 b'_{11}}([R_f\theta^2 D]_1 b'_{11} - [R_f\theta^2 D]_2 b'_{21}) + e^{\Delta Q_1 b'_{12}}([R_f\theta^2 D]_2 b'_{21} - [R_f\theta^2 D]_1 b'_{12})} \tag{35}$$

where b'_{11}, b'_{12}, and b'_{21} are the steady state forms of the coefficients defined in Eq. (29) (given in Eq. (A1) in Appendix A).

Since $b'_{11} \ll b'_{12}$, then $e^{b'_{11}\Delta Q_1} \ll e^{b'_{12}\Delta Q_1}$ and Eq. (35) can be approximated by the following,

$$f_{2STD}(Q_2) = \frac{[R_f\theta^2 D]_1 C_o(b'_{11} - b'_{12})e^{\Delta Q_1 b'_{11}+b'_{21}Q_2}}{[R_f\theta^2 D]_2 b'_{21} - [R_f\theta^2 D]_1 b'_{12}} \tag{36}$$

and from Eq. (32), for a prescribed flux and zero initial conditions,

$$f_{2STD}(Q_2) = \frac{q_{co}e^{\Delta Q_1 b'_{11}+b'_{21}Q_2}[b'_{12} - b'_{11}]}{(q_{o1} - [R_f\theta^2 D]_1 b'_{11})\left[b'_{12} - \dfrac{[R_f\theta^2 D]_2 b'_{21}}{[R_f\theta^2 D]_1}\right]} \tag{37}$$

2.3.1. Numerical Laplace inversion

In order to find the concentration with respect to time using Eqs. (31) and (32) the de Hoog algorithm (de Hoog et al., 1982) was used to numerically invert from Laplace space. With this procedure, the function is evaluated at a number of locations in Laplace space and these values used to calculate the inverse.

In this paper the semi-analytical finite domain two-layer solution will be tested by comparison with an equivalent numerical analysis calculated using SWIMv2 (Verburg et al., 1996).

2.4. Steady state water content profile

In order to move from Q to z space requires the water content and retardation factor depth profiles at the time of interest. Earlier it was reasoned that transient variations in water movement in response to climate were smoothed as water moves through the unsaturated profile, such that, as an approximation, the water content profile at depth is a result of the average of the surface conditions. Various steady state solutions to unsaturated water movement have been derived (e.g. Gardner, 1958). Here a simple solution is presented that allows for layering and root water uptake.

Within the root zone, conservation of water mass can be written as,

$$\frac{dq}{dz} = S_{wa} \tag{38}$$

Below the root zone $S_{wa} = 0$.

Eq. (38) can be integrated to,

$$q = S_{wa}z + q_o \tag{39}$$

Substitution of the Buckingham–Darcy relation for the water flux leads to,

$$K(h)\left[\frac{dh}{dz} - 1\right] = -S_{wa}z - q_o \tag{40}$$

With the transform variable, $h' = h - z$, Eq. (40) becomes,

$$K(h' + z)\frac{dh'}{dz} = -S_{wa}z - q_o \tag{41}$$

With the hydraulic conductivity defined by,

$$K(h) = K_s e^{\alpha_g h} \tag{42}$$

Eq. (41) can be re-written as,

$$\int_{h'}^{h'_L} K_s e^{\alpha_g \bar{h}'} d\bar{h}' = -\int_z^{z_L} [S_{wa}\bar{z} + q_o]e^{-\alpha_g z} dz \tag{43}$$

Integrating Eq. (43) leads to the following,

$$h = \frac{1}{\alpha_g}\ln\left[e^{\alpha_g(h_L+z-z_L)} + \frac{1}{K_s}\left(\frac{S_{wa}}{\alpha_g} + S_{wa}z + q_o - e^{\alpha_g(z-z_L)}\left[\frac{S_{wa}}{\alpha_g} + S_{wa}z_L + q_o\right]\right)\right] \tag{44}$$

Eq. (44) relates matric potential to depth for a constant root water uptake. Layering (that can allow for vertical variation in hydraulic properties and root water uptake) can be incorporated by using Eq. (44) for each layer and solving upwards from the watertable, at which $h_L = 0$, and equating h at the top of each layer with the overlying layer's h_L.

The use of Eq. (42) for the hydraulic conductivity is an approximation. Philip (1969) noted that "even though it cannot be claimed that [Eq. (42)] is universally exact, it does model in a reasonably convincing way the quite generally observed rapid non-linear decrease with h."

The water content profile is required in order to use the Q transformed transport equation presented above. The matric potential profile defined by Eq. (44) can be used with the moisture retention relationship, $\theta(h)$, to calculate the moisture content profile. The van Genuchten moisture retention relation can be written as (van Genuchten, 1980),

$$\frac{\theta - \theta_r}{\theta_s - \theta_r} = \frac{1}{\left[1 + \left(\frac{h}{h_g}\right)^n\right]^m} \tag{45}$$

where $m = 1 - 1/n$.

3. Testing of 2-layer solution

3.1. Accuracy of de Hoog inversion

The accuracy of the de Hoog numerical Laplace inversion is partly related to the number of inversion points at which the function is calculated. A first sep in the application of the 2-layer solution is determining the number of function evaluations in the inversion that yield the greatest mathematical accuracy. This was done by comparing the 2-layer results (using vertically uniform properties) with an equivalent analytical solution to the advection–dispersion equation for a range of numbers of function evaluations. The analytical solution that was used in this analysis comes from Bear (1979) and is for a semi-infinite domain with a fixed surface concentration and a constant vertical water flux,

$$c(z,t) = \frac{c_s}{2}\exp\left(\frac{qz}{2\theta D}\right) \times \left\{ e^{-vz}\operatorname{erfc}\left[\frac{z - t/\theta R_f\sqrt{q^2 - 4\mu\theta^2 D}}{2\sqrt{Dt/R_f}}\right] + e^{vz}\operatorname{erfc}\left[\frac{z + t/\theta R_f\sqrt{q^2 - 4\mu\theta^2 D}}{2\sqrt{Dt/R_f}}\right]\right\} \tag{46}$$

where

$$v = \sqrt{\left(\frac{q}{2\theta D}\right)^2 - \frac{\mu}{D}}$$

where q is the uniform, profile constant water flux.

Fig. 1 presents the differences between the results of Eq. (46) and those calculated using the 2-layer solution, Eq. (12) with coefficients defined by Eqs. (13)–(15),(21), and (22) for a conservative, non-reactive solute at several times for a surface concentration of 1, $q = 0.1$ cm/h, $\alpha_L = 1$, a problem domain of 200 cm, and volumetric water content set to 1. The use of this water content is not intended to be physically realistic, but in this hypothetical test, since there is no degradation, its only influence is on the transport velocity through the ratio q/θ. Thus the transport velocity is equal to the water flux of 1 cm/h, a rate that, in a very broad sense, is appropriate for field soils.

In Fig. 1 the differences between the analytical results (Eq. (46)) and those involving the numerical Laplace inversion are consistently minimized for 210 function evaluations in the de Hoog inversion.

3.2. Testing with transient water movement

In the derivation presented above it was proposed that the advective migration of solute could be represented using the averages of the surface and transpiration fluxes. This is a significant approximation to a complex, dynamic process. For a soil exposed to climate, rainfall occurs as distinct events interspersed with periods of transpiration. The accuracy of a steady state approach for explaining the water movement behaviour in the 2-layer solution is largely dependent on flow at depth being slow in its response and due more to the average of the surface processes than event related. This will be directly

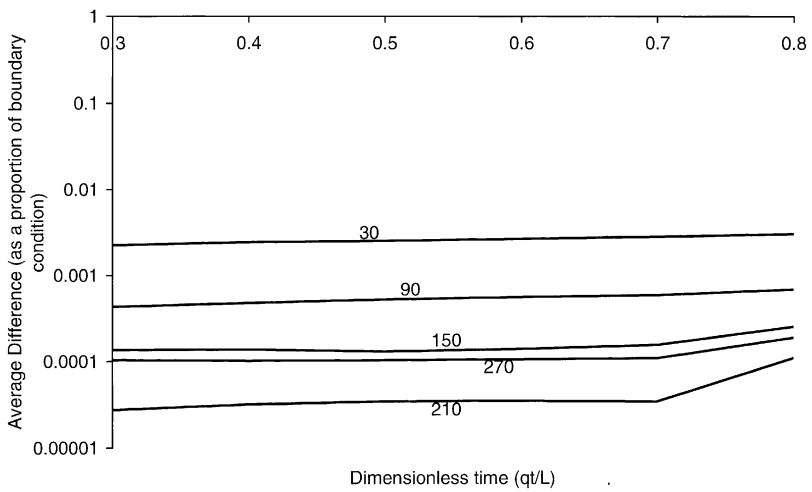

Fig. 1. Accuracy of the de Hoog numerical Laplace inversion. The difference between analytical (using Eq. (46)) and 2-layer results calculated using de Hoog inversion with respect to dimensionless time and number of function evaluations in the de Hoog inversion.

related to the rate of water migration, the result of a combination of event magnitudes and hydraulic properties.

The accuracy of the 2-layer solution using the average surface and transpiration fluxes with steady-state water movement will be investigated using hypothetical simulations. The basis of comparison for these analyses will be the SWIMv2 model of Verburg et al. (1996) that numerically solves the advection–dispersion equation coupled to Richards' equation. In the SWIM simulations the van Genuchten moisture retention relationship was used with the Mualem hydraulic conductivity function. Fig. 2 presents the cumulative water infiltration and transpiration imposed in the SWIM simulations. In a manner intended to replicate natural conditions, infiltration is composed of a series of discrete events of varying magnitude and time of separation. Transpiration is applied in a more continuous fashion but still varying through time. To appreciate the role of the hydraulic properties on the accuracy of the 2-layer solutions two sets of the properties are used (see Table 1); Grenoble

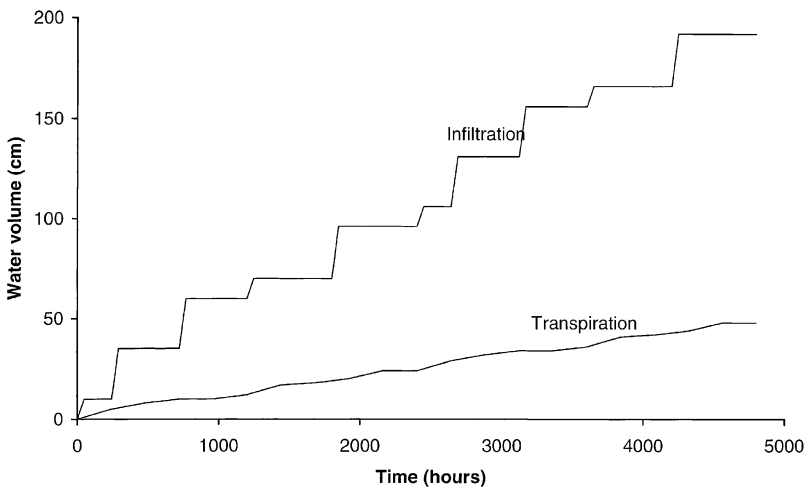

Fig. 2. Surface boundary conditions used for the SWIMv2 simulations. The infiltration and transpiration expressed here as cumulative water volumes through time.

Table 1
Soil hydraulic properties used in model simulations (properties for Grenoble sand are from Fuentes et al. (1992); Guelph loam properties are from van Genuchten (1980))

	θ_s(cm^3/cm^3)	θ_r(cm^3/cm^3)	K_s(cm/h)	h_g(cm)	m	α_g(cm^{-1})
Grenoble sand	0.312	0.0	15.32	−16.39	0.2838	0.09
Guelph loam	0.434	0.218	1.32	−50	0.275	0.12

sand has a high permeability, while Guelph loam is less permeable.

The simulations were for a vertical column of 10 m with vertically uniform hydraulic properties and a root zone of 50 cm. The initial water content profile for SWIMv2 was calculated using the steady state solution, Eq. (44), with the average of the infiltration and transpiration time series.

The mathematical accuracy of the solution procedures used in SWIMv2 has been extensively established with over 50 publications using it and closely related versions (see Verburg et al. (1996) for a listing). Therefore there is no need to re-establish this mathematical accuracy in this paper, however the model's behaviour with respect to the number of nodes will be investigated in order to identify the appropriate discretization for the subsequent simulations. In Fig. 3 the concentration profiles at two times are presented for two simulations using the surface driving conditions presented in Fig. 2 and the Grenoble sand properties in Table 1. These two simulations involve spatial discretizations with 100 and 250 nodes, respectively, for the 10 m profile described above. There are no discernable differences between the results presented for the two spatial discretizations. In the subsequent SWIMv2 simulations 250 nodes were used to maximize the spatial resolution of the results of flow and transport solutions.

3.2.1. Guelph loam hydraulic properties

Fig. 4 presents the vertical solute concentration profile at several times for transport in soil with Guelph loam hydraulic properties under the infiltration and transpiration time series presented in Fig. 2. Each profile is calculated using the average flux over the time of interest, i.e. for 2400 h the average flux is calculated from the infiltration and transpiration up to that time, with the steady state water content profile calculated at each time level with the fluxes for that time. In Fig. 5 the range of water content variation is presented with the average, maximum and minimum vertical water content profiles from the SWIM results compared with the steady state water content profile calculated with Eq. (44).

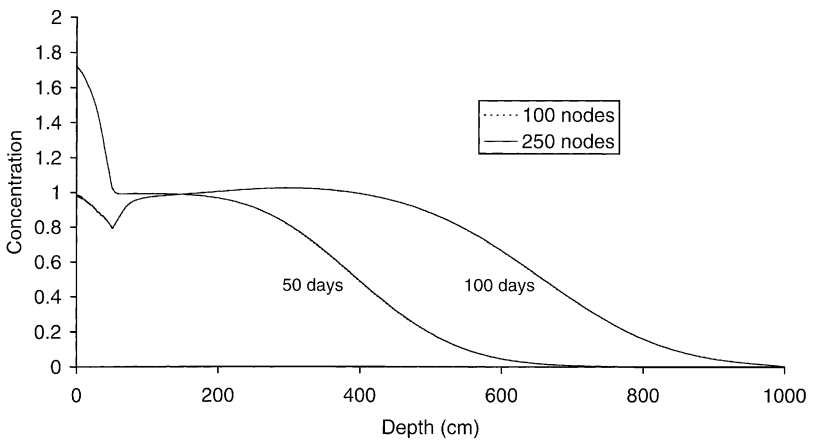

Fig. 3. Effect of the number of nodes in the SWIMv2 solution for solute concentration. Concentrations are presented for two times and with simulations involving 100 and 250 nodes. The surface conditions presented in Fig. 2 were used as the surface boundary conditions for the simulations and Grenoble sand hydraulic properties were used.

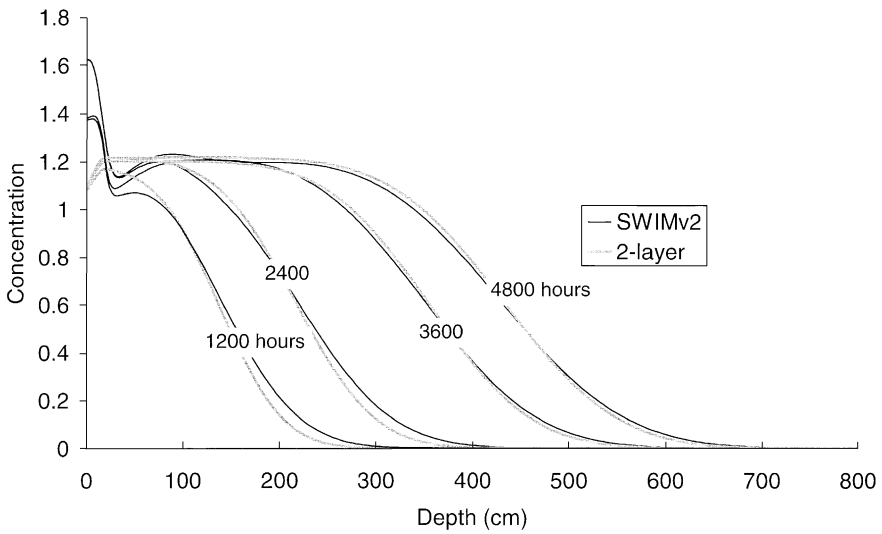

Fig. 4. Solute concentration variation with depth from the SWIMv2 and 2-layer simulations for Guelph Loam hydraulic properties and with the water boundary conditions as given in Fig. 2. The depth profiles are presented for four evenly spaced times. The 2-layer results are calculated using the averages of the water boundary conditions up to the time presented.

In terms of the position of the solute front, the SWIM and 2-layer solution results are consistently close as the front moves down the soil profile, even for early times when the infiltration and transpiration time series has been highly heterogeneous. This supports the use of average surface water fluxes, calculated at each time of interest, and the use of the steady state solution for the water content profile to transform from Q to z space. While the front positions are close they are more dispersed than the two layer results, particularly for the early time profiles, at 1200 and 2400 h. One explanation for this is that the SWIM

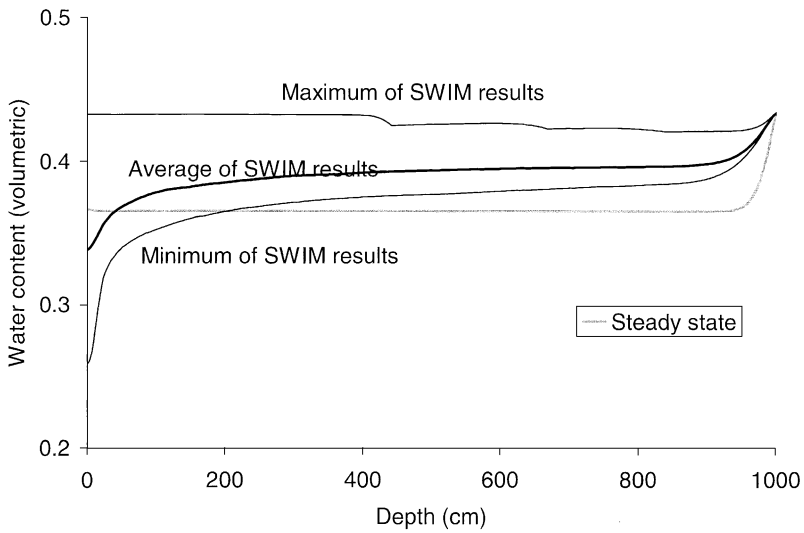

Fig. 5. The range of variation in water content from the SWIMv2 simulations for Fig. 3 compared with the steady-state solution for the water content results used with the 2-layer results. The overall maximum, minimum and average water content profiles from SWIMv2 are presented.

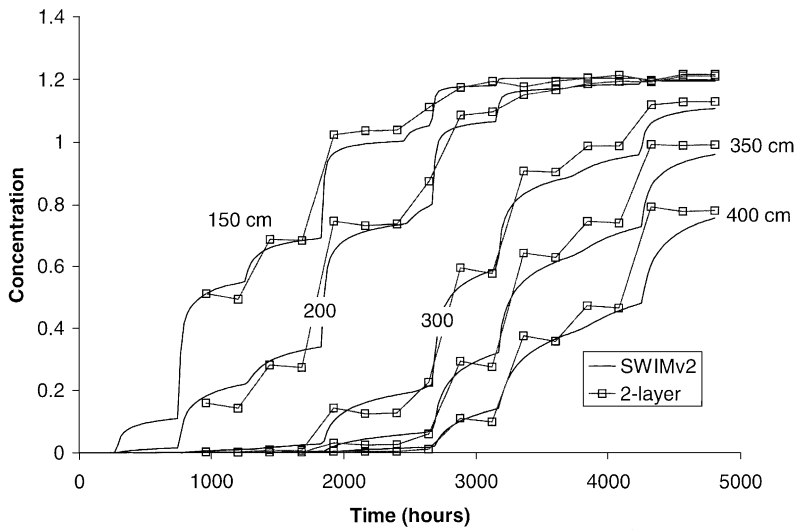

Fig. 6. A comparison between the SWIMv2 and 2-layer solution solute concentration results with time at a number of depths for Guelph loam hydraulic properties. The simulations are the same as those presented in Fig. 4 with the surface boundary conditions presented in Fig. 2. The 2-layer results are calculated using the average of the water flux up to the time of interest.

water content profile tends to be changing rapidly with depth up to around 300 cm. With the 2-layer result the transformation from Q to z space is based on the nearly flat steady state water content profile presented in Fig. 5. This will act to 'compress' the solute front in z space relative to the SWIM results. At greater depths the average SWIM water content and steady state profiles are relatively flat with a similar rate of change. At these depths the concentration profiles are in close agreement.

Fig. 6 presents the solute concentration variation with time, for the two approaches, at a series of

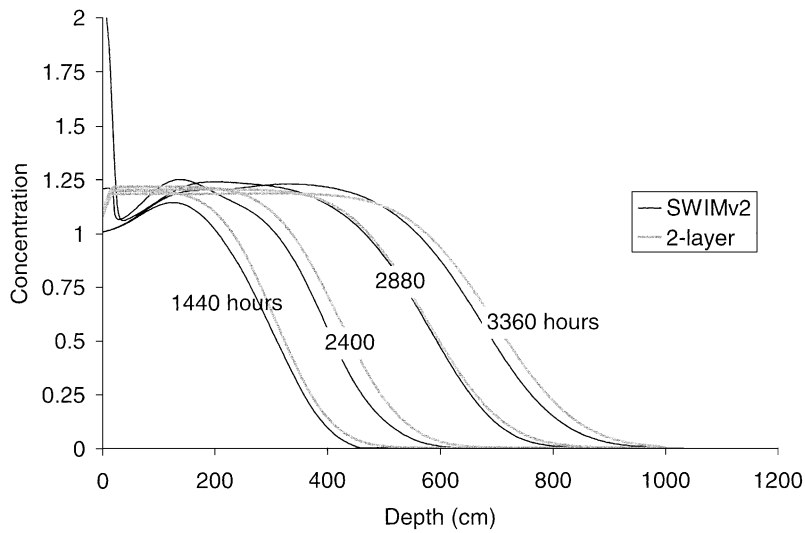

Fig. 7. Solute concentration variation with depth calculated using Grenoble sand hydraulic properties. SWIMv2 results are compared with those of 2-layer solution and use the surface water fluxes presented in Fig. 2. The 2-layer results are based on using the average of the surface water fluxes up to the time of interest.

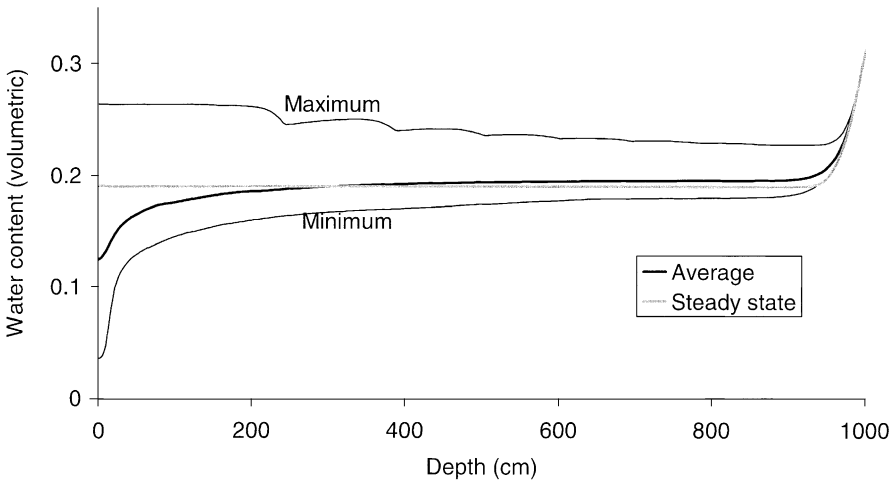

Fig. 8. The range of variation in water content from the SWIMv2 simulations for Fig. 7 is compared with the steady-state solution for water content profile used with the 2-layer results. The overall maximum, minimum and average water content profiles from SWIMv2 are presented.

depths. Each 2-layer result is calculated using the average of the infiltration and transpiration fluxes up to the time of interest. In general the results from the two procedures are in close agreement. Both sets of results show strong, infiltration event related, pulses of solute moving past the selected depths. The SWIM results show how these pulses become more dispersed the deeper they travel. The 2-layer solution does not accurately represent this dispersion behaviour, a consequence of using the steady water assumption with average water fluxes. However, the results from the two approaches converge rapidly following the arrival of each pulse.

3.2.2. Grenoble sand hydraulic properties

Fig. 7 presents the vertical solute concentration profiles at several times from SWIMv2 and the 2-layer solution. The vertical water content profiles from SWIM (the average, maximum and minimum) and the steady states solution are presented in Fig. 8.

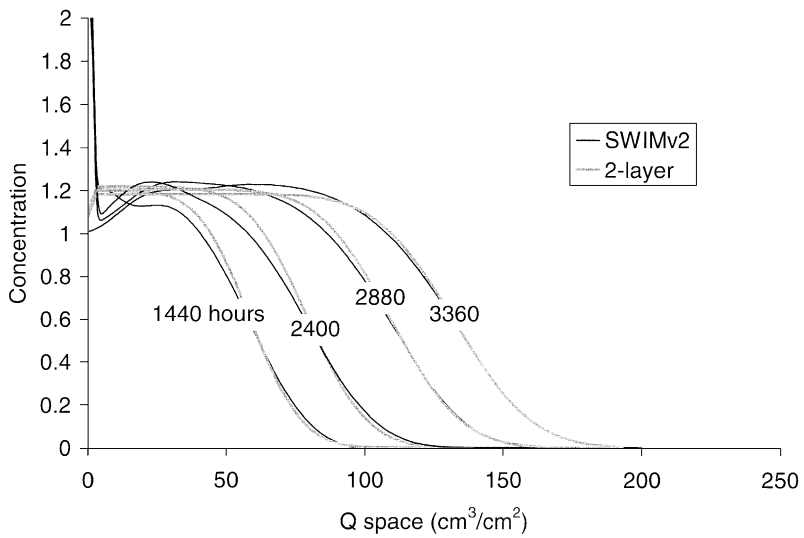

Fig. 9. Solute concentration results from Fig. 7 presented in Q space. In Q space, differences in solute concentration as a result of differences in the approaches to explaining water movement in SWIMv2 and the 2-layer solution are reduced.

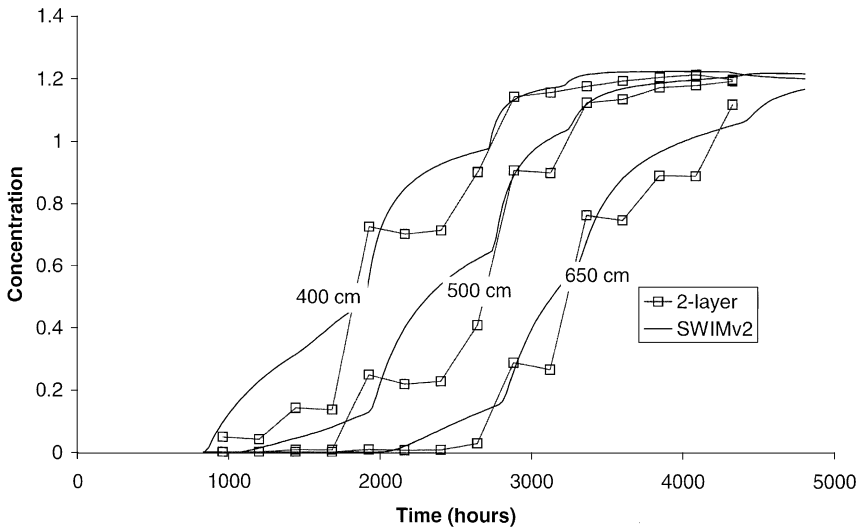

Fig. 10. A comparison between the solute concentration results with time calculated using SWIMv2 and the 2-layer solution. These simulations used Grenoble sand hydraulic properties and the surface boundary conditions presented in Fig. 2. The 2-layer results are calculated using the average of the water flux up to the time of interest.

While the shapes of the solute fronts are very close for the two procedures, the front positions are not as close as for the Guelph loam simulations presented above. This could be a result of inaccuracies in the use of the averaged surface water fluxes for the advective flux or the use of the steady state water solution in the Q to z space transformation. Fig. 9 presents the same concentration results as Fig. 7 in Q space. In Q space the positions of the solute front are in much closer agreement, indicating that the inaccuracies in front position evident in Fig. 7 are a result of using the steady state approximation in the Q to z transformation. Grenoble sand has a high hydraulic conductivity; infiltration events lead to pulses of water and solute that travel rapidly down the soil profile. In addition there is a wide range over which the water content varies in response to infiltration and transpiration, so while the average and steady state water content profiles are close over most of the profile in Fig. 8, at a particular time there could be significant differences.

Another aspect to this rapid flow behaviour is the difference in the solute concentration below the root zone and behind the front. At each time level the concentration for this region is either slightly above the 2-layer solute results or less than these, as the solute concentration over the vertical profile is affected by the current state at the surface. The 2-layer solution therefore represents the average response. This conclusion is supported by the results in Fig. 10 where the solute concentration at several depths over time is presented for the 2-layer solution and SWIM. For these simulations the 2-layer and the steady state water content solutions are calculated at series of times using the average infiltration and transpiration up to that time. While the 2-layer results fail to represent the true arrival and temporal dispersion of the solute pulses, as with Guelph loam properties there is good overall agreement.

Within the root zone solute concentration is significantly affected by the current surface conditions and, due to the use of averaged water movement, the 2-layer solution cannot reliably estimate this behaviour.

4. Discussion and conclusions

This paper investigates the use of analytical solutions for unsaturated solute migration, and presents a simple approach for calculating the transport of contaminants to groundwater that could prove

suitable for risk mapping. Root zone processes are represented including water loss due to plant transpiration that can act to concentrate solutes that the excluded by the root system. In addition, higher organic matter contents, microbial populations and oxygen concentrations within the root zone lead to solute transport properties that are different to the rest of the soil profile. In the solution presented in this paper, the unsaturated profile is divided into two layers, with the upper layer to represent the root zone effects. A common assumption made with existing analytical solutions to the advection–dispersion equation is that the soil profile is homogeneous and thus the localised effect of root zone processes is not accurately represented.

An interesting aspect to the approach presented in this paper is how water movement is characterised in the solute transport solution. The solutions are based on the Q transformed advection–dispersion equation (Eq. (8)) where, for a conservative solute, the water movement properties are the averages of the infiltration rate (q_o) and the transpiration rate (S_{wa}). However, in order to invert from Q space back to depth, z, requires the water content profile, but only at the same time that the concentration is required. In the paper, a steady-state water content profile was used to invert from Q space. However, it is also possible to base the Q to z space inversion on direct field measurement of the water content profile. This, along with measurement of the average infiltration and transpiration rates for the period of interest, would allow the solute transport to be calculated without a water flow solution.

The underlying assumption in the water movement modelling, and some aspects of the solute transport modelling, is that the unsaturated profile behaves as a porous medium. However, in many soils and aquifer structures macropores exist that allow preferential flow, and this deviates from the porous media assumptions. Preferential flow can be an important process since it has the potential to provide a rapid pathway for contaminants to reach the watertable. A complication with representing preferential flow is that transport within the macropores can be linked to the surrounding matrix. In some situations, while water may move rapidly, solutes are lost to the matrix and the net vertical migration of chemicals is effectively retarded by this matrix diffusion (as with the Chalk of northern Europe). The model presented here would have to be modified to represent this preferential flow and matrix diffusion process, possibly along the lines of the dual porosity approach of Hantush et al. (2002). However, if the preferential flow involves no significant matrix diffusion then the method presented in this paper could still be used with appropriate water fluxes and porosities.

One of the key obstacles in the application of any process based approach, such as that proposed in this paper, is the estimation of the location specific properties that affect transport. To replicate the area covered by existing vulnerability maps would involve estimating very large sets of properties. Some of these are physico-chemical characteristics, such as the organic carbon content that could play a role in the transport of a large number of substances. While others could be site and contaminant specific, such as the degradation rate which can be affected by the oxygen concentration. While we are improving our knowledge of these properties through various efforts, it must be recognised that they will only ever be known with a degree of uncertainty. It may be that many can be estimated from similar situations or, at best, through expert opinion. Therefore, inherent in any mapping approach must be a treatment of parameter uncertainty; this would allow an estimate of the probability that regulatory limits could be exceeded and this would then be the property mapped.

Overall, the accuracy of the combined approach of two-layer transport equation and semi-steady state water movement is a function of the soil hydraulic properties and the depth of observation. The procedure had greater accuracy for the Guelph loam soil hydraulic properties than for the more permeable Grenoble sand properties. For Grenoble sand it was shown that while the use of the averages of the infiltration and transpiration rates without any temporal resolution of the behaviour of these properties could lead to very close agreement in the Q transform space, the use of the steady water movement solution introduced differences. These differences arose from the highly transient nature of water movement for this soil, with the vertical water profile being strongly influenced by infiltration events. For this soil, the steady state solution tended to smooth out wetting fronts and thus not represent the true arrival of the associated pulses of solute. However, this inaccuracy became less with depth, such that at a depth of 650 cm the two-layer results were close to the numerical.

Therefore, for highly permeable soils the approach of steady state water movement with the two-layer solution can provide useful solute transport results for deeper profiles. More work is required to determine the relationship between accuracy, profile depth, climate, and hydraulic properties.

The accuracy of the developed procedure will therefore be strongly linked to the depth to watertable. For areas with a shallow watertable and permeable soils the model results will be approximate and more sensitive modelling procedures will be required to accurately represent the aquifer vulnerability. However, for deeper watertables the approach is shown to be accurate and offers an efficient approach to estimating the vulnerability.

Another aspect to the 2-layer solution is that it allows for time varying surface boundary conditions for solute concentration or flux. Thus the seasonal loading that occurs with fertiliser or pesticide application, for example, can be represented.

Various forms of the two-layer solution were presented. One solution described solute transport in the finite domain represented by the soil surface and the watertable. With this the groundwater had a fixed concentration, unaffected by the solute arriving from the unsaturated zone. In reality solute would disperse through the receiving aquifer and the lower boundary on the two-layer solution would be a function of the rate of this dispersion. The current form, if the lower boundary has a fixed concentration, is therefore approximate and represents the situation where the solute is transported away from the watertable at a much greater rate than at which material arrives. However, the lower boundary concentration can be a function of time, which would allow more sophisticated representations of the aquifer dispersion.

A much simpler form of solution was derived for the semi-infinite domain. While this solution neglects the effect of the watertable as possible boundary to the flow system, it could be used to represent the concentration of solute arriving at some critical depth. An example of this is the watertable where regulatory limits on contaminant concentration are often applied.

The most appropriate basis for a risk or vulnerability mapping procedure would be the steady-state form of the semi-analytical solutions (Eqs. (36) or (37)). These simple relations are analytic and would provide a means of efficiently calculating the risk (for example; the probability of exceeding a regulatory limit). A risk calculation would mean that the transport relation would have to be combined with a treatment for parameter uncertainty like Monte Carlo or approximate procedures such as first-order second moment (Dettinger and Wilson, 1981).

Acknowledgements

This work was supported by UK Engineering & Physical Sciences Research Council grants GR/N33119 and GR/R86911.

Appendix A

Steady-state form of coefficients defined in Eq. (29),

$$b'_{i1} = \frac{\beta_i - \sqrt{\beta_i^2 - 4\alpha_i\gamma_i}}{2\alpha_i} \quad \text{and}$$
$$b'_{i2} = \frac{\beta_i + \sqrt{\beta_i^2 - 4\alpha_i\gamma_i}}{2\alpha_i} \tag{A1}$$

References

Aller L., Bennett T., Lehr J.H., Petty R.J., Hackett G., 1987. Drastic: a standardised system for evaluating groundwater pollution potential using hydrographic settings, US-EPA Report 600/2-87-035.

Barry, D.A., Sposito, G., 1989. Analytical solution of a convection–dispersion model with time-dependent transport coefficients. Water Resour. Res. 25 (12), 2407–2416.

Bear, J., 1979. Hydraulics of Groundwater, Mc-Graw Hill, New York.

Bond, W.J., Smiles, D.E., 1983. Influence of velocity on hydrodynamic dispersion during unsteady flow. Soil Sci. Soc. Am. J. 47 (3), 438–441.

Bosma, W.J.P., van der Zee, S.E.A.T.M., 1992. Analytical approximation for nonlinear adsorbing solute transport in layered soils. J. Hydrol. 10, 99–118.

Connell, L.D., 2002. A simple analytical solution for unsaturated solute migration under dynamic water movement conditions and zone effects. Geol. Soc., Lond., Special Public. 193, 255–264.

Connell, L.D., Haverkamp, R., 1996. A semi-analytical model for soil solute movement under plant water use. Soil. Sci. Soc. Am. J. 60 (5), 1350–1355.

Dettinger, M.D., Wilson, J.L., 1981. First-order analysis of uncertainty in numerical models of groundwater flow.

I. Mathematical development. Water Resour. Res. 17 (1), 149–161.

Elrick, D.E., Mermoud, A., Monnier, T., 1994. An analysis of solute accumulation during steady-state evaporation in an initially contaminated soil. J. Hydrol. 155, 27–38.

Foster, S.S.D., 1987. Fundamental concepts in aquifer vulnerability, pollution risk and protection strategy. TNO Committee for Hydrological Research: Proceedings and Information 38, 36–86.

Fuentes, C., Haverkamp, R., Parlange, J.-Y., 1992. Parameter constraints on closed-form soil water relationships. J. Hydrol. 134, 117–142.

Gardner, W.R., 1958. Some steady state solutions of the unsaturated moisture flow equation with application to evaporation from a water table. Soil Sci. 85, 228–232.

van Genuchten, M.Th., 1980. A closed form equation for predicting the hydraulic conductivity of unsaturated soils. Soil Sci. Soc. Am. J. 44, 892–898.

van Genuchten, M.T., Dalton, F.N., 1986. Models for simulating salt movement in aggregated field soils. Geoderma 38, 165–183.

Hantush, M.M., Marino, M.A., Islam, M.R., 2000. Models for leaching of pesticides in soils and groundwater. J. Hydrol. 227, 66–83.

Hantush, M.M., Govingaraju, R.S., Marino, M.A., Zhang, Z., 2002. Screening model for volatile pollutants in dual porosity soils. J. Hydrol. 260, 58–74.

de Hoog, F.R., Kinght, J.H., Stokes, A.N., 1982. An improved method for numerical Laplace inversion of Laplace transforms. SIAM J. Sci. Stat. Comput. 3 (3), 357–366.

Jury, W.A., Grsruber, J., 1989. A stochastic analysis of the influence of soil and climatic variability on the estimate of pesticide groundwater pollution potential. Water Resour. Res. 25 (12), 2465–2474.

Khan, M.A., Liang, T., 1989. Mapping pesticide contamination potential. Environ. Mgmt 13, 233–242.

Leonard, R.A., Knisel, W.G., Still, D.A., 1987. Gleams: groundwater loading effects of agricultural management systems. Trans. ASCE 30, 1403–1418.

Philip, J.R., 1969. Theory of infiltration. Adv. Hydrosci. 5, 215–296.

Rao, P.S.C., Hornsby, A.G., Jessup, R.E., 1985. Indices for ranking the potential for pesticide contamination of groundwater. Soil Crop Sci. Soc. Fla. Proc. 44, 1–4.

Sun, Y., Petersen, J.N., Clement, T.P., 1999. Analytical solutions for multiple species reactive transport in multiple dimensions. J. Contam. Hydrol. 25, 429–440.

Verburg K., Ross P.J., Bristow K.L., 1996. SWIMv2.1 User Manual, CSIRO, Divisional Report No. 130.

Wagenet, R.J., Hutson, J.L., 1986. Predicting the fate of nonvolatile perticides in the unsaturated zone. J. Environ. Qual. 15, 315–322.